Journal Name

ARTICLE TYPE

Cite this: DOI: 10.1039/xxxxxxxxxx

Highly Polarization-Sensitive, Visible-blind and Self-powered Ultraviolet Photodetection Based on Two-Dimensional Wide Bandgap Semiconductors: A Theoretical Prediction

Yongzhi Luo,[a] Yibin Hu,[b] Yiqun Xie,*[a]

Received Date
Accepted Date

DOI: 10.1039/xxxxxxxxxx

www.rsc.org/journalname

In the following pages, we give the electronic and optical properties, as well as the photocurrent for sixteen 2D WBG semiconductors, as mentioned in the main text.

[a] *Department of Physics, Shanghai Normal University, 100 Guilin Road, Shanghai 200232, P.R. of China. E-mail: yqxie@shnu.edu.cn*
[b] *State Key Laboratory of Infrared Physics, Shanghai Institute of Technical Physics, Chinese Academy of Sciences, Shanghai 200083, P.R. of China.*

Electronic Supplementary Information (ESI)

Electronic band structures of $CdCl_2$ (a) and CdI_2 (b)

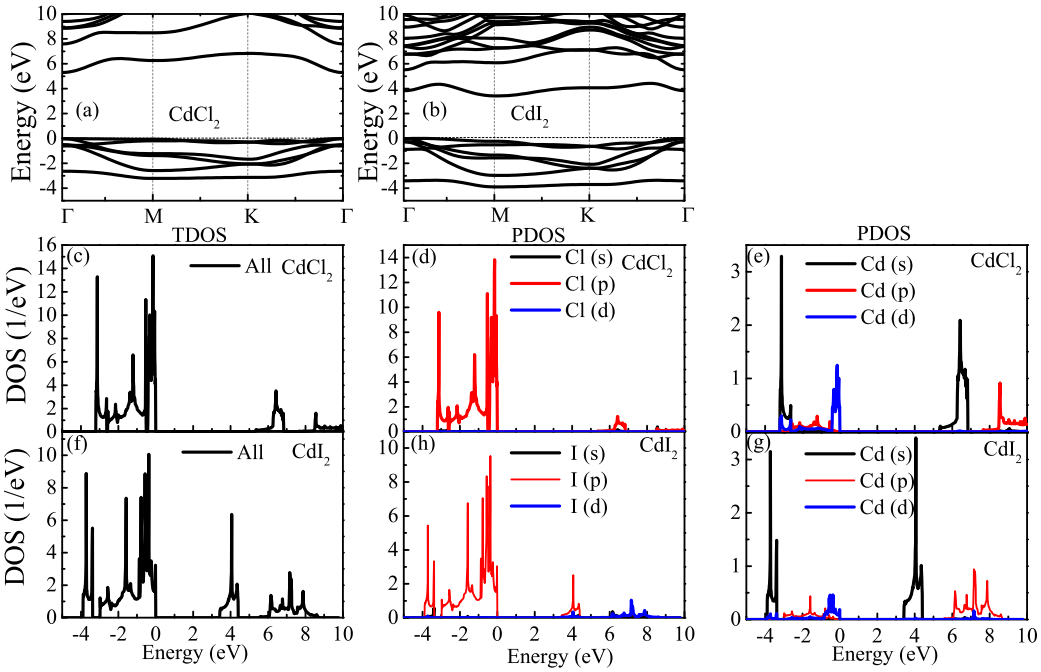

Fig. S1 Electronic band structures of the monolayer $CdCl_2$ (a) and CdI_2 (b) calculated from the HSE06 hybrid functional. Fermi energy level set at zero. TDOS and PDOS for $CdCl_2$ (c,d,e) and CdI_2 (f,h,g).

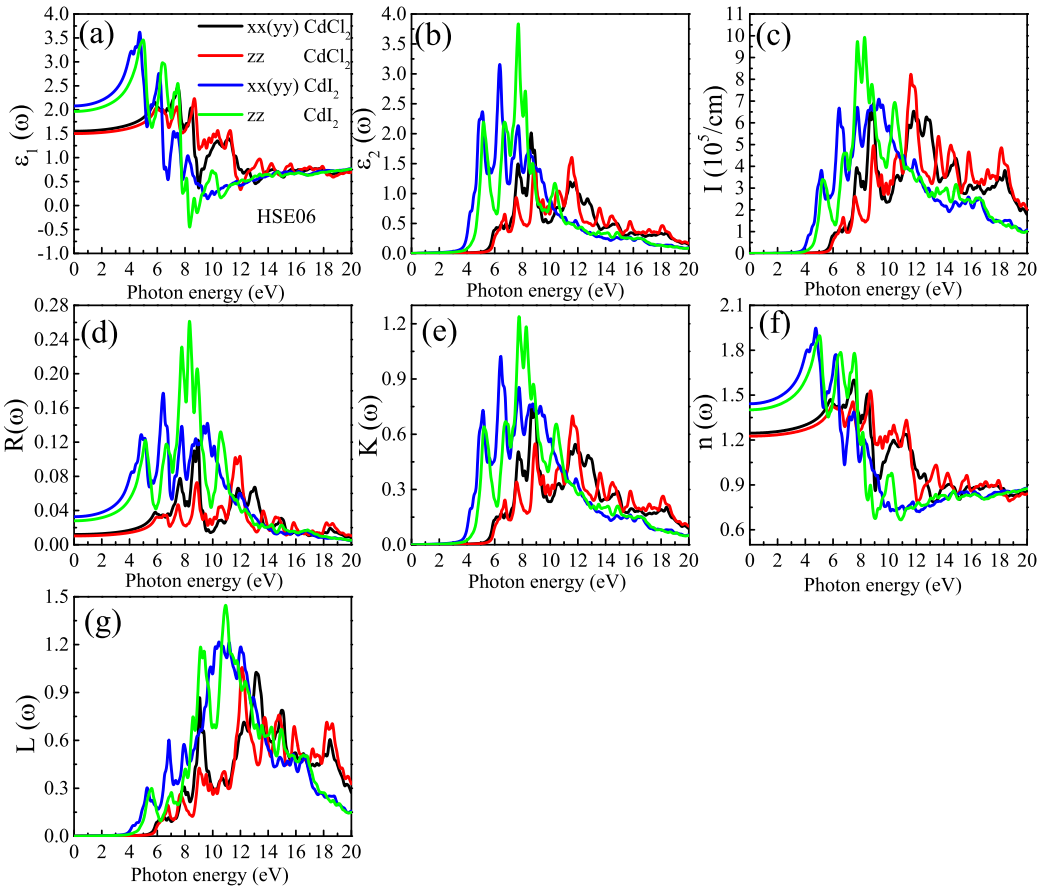

Fig. S2 Optical properties of the monolayer CdX_2 (X = Cl, I). The real $\varepsilon_1(\omega)$ (a) and imaginary parts $\varepsilon_2(\omega)$ (b) of the complex dielectric function; absorption coefficient I(ω) (c); reflectivity R(ω) (d); extinction coefficient K(ω)(e); refractive index n(ω) (f) and energy loss spectrum L(ω) (g). The unit of absorption coefficient is 10^5/cm. "xx", "yy" and "zz" represent the polarization of light along the x (**E**$\perp z$), y (**E**$\perp z$) and z (**E**//z) directions respectively.

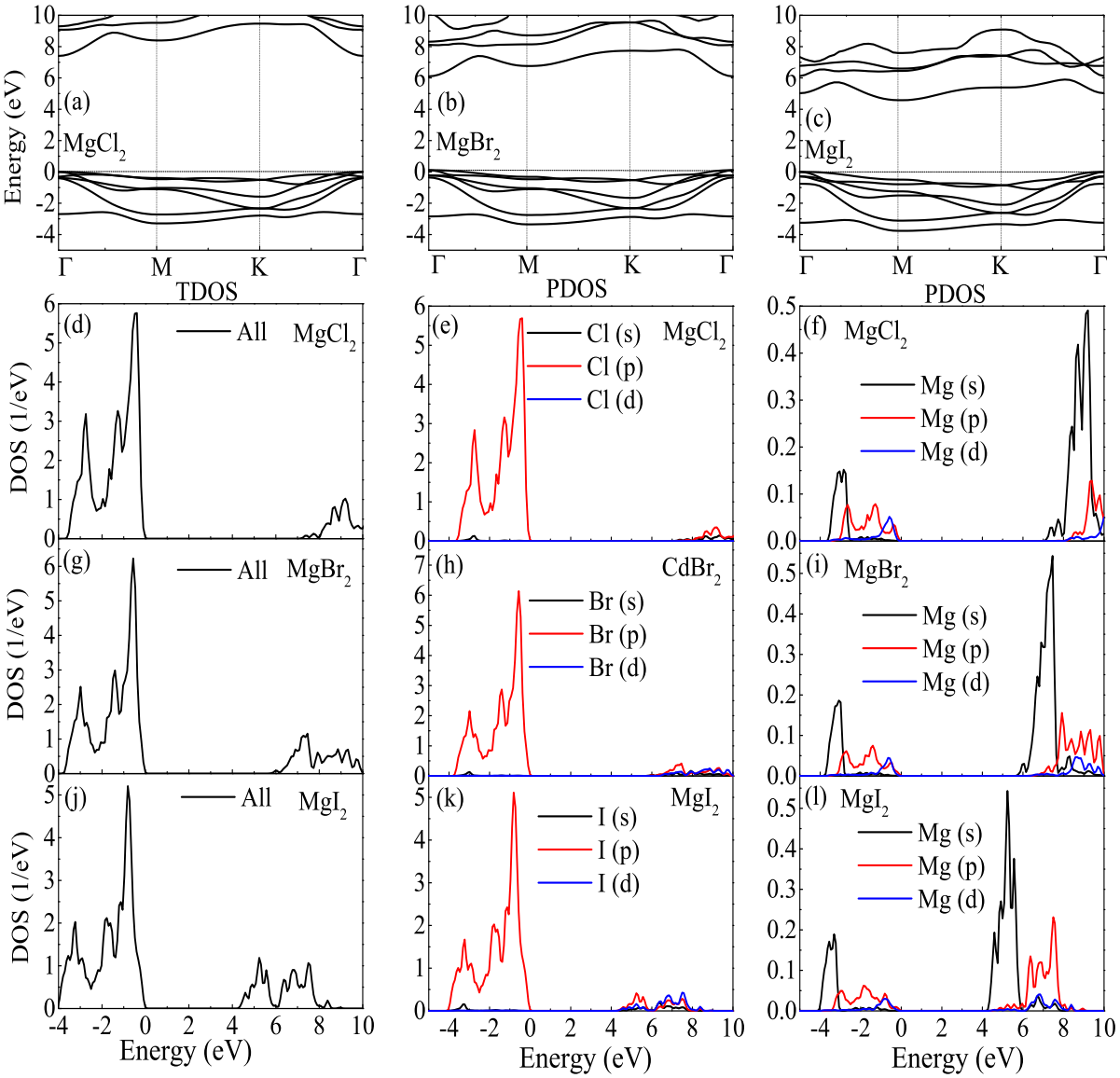

Fig. S3 Electronic band structures of $MgCl_2$ (a), $MgBr_2$ (b) and MgI_2 (c) from the HSE06 calculations. TDOS and PDOS for $MgCl_2$ (d,e,f), $MgBr_2$ (g,h,i) and MgI_2 (j,k,l).

Optical peoperties structures of MgX_2

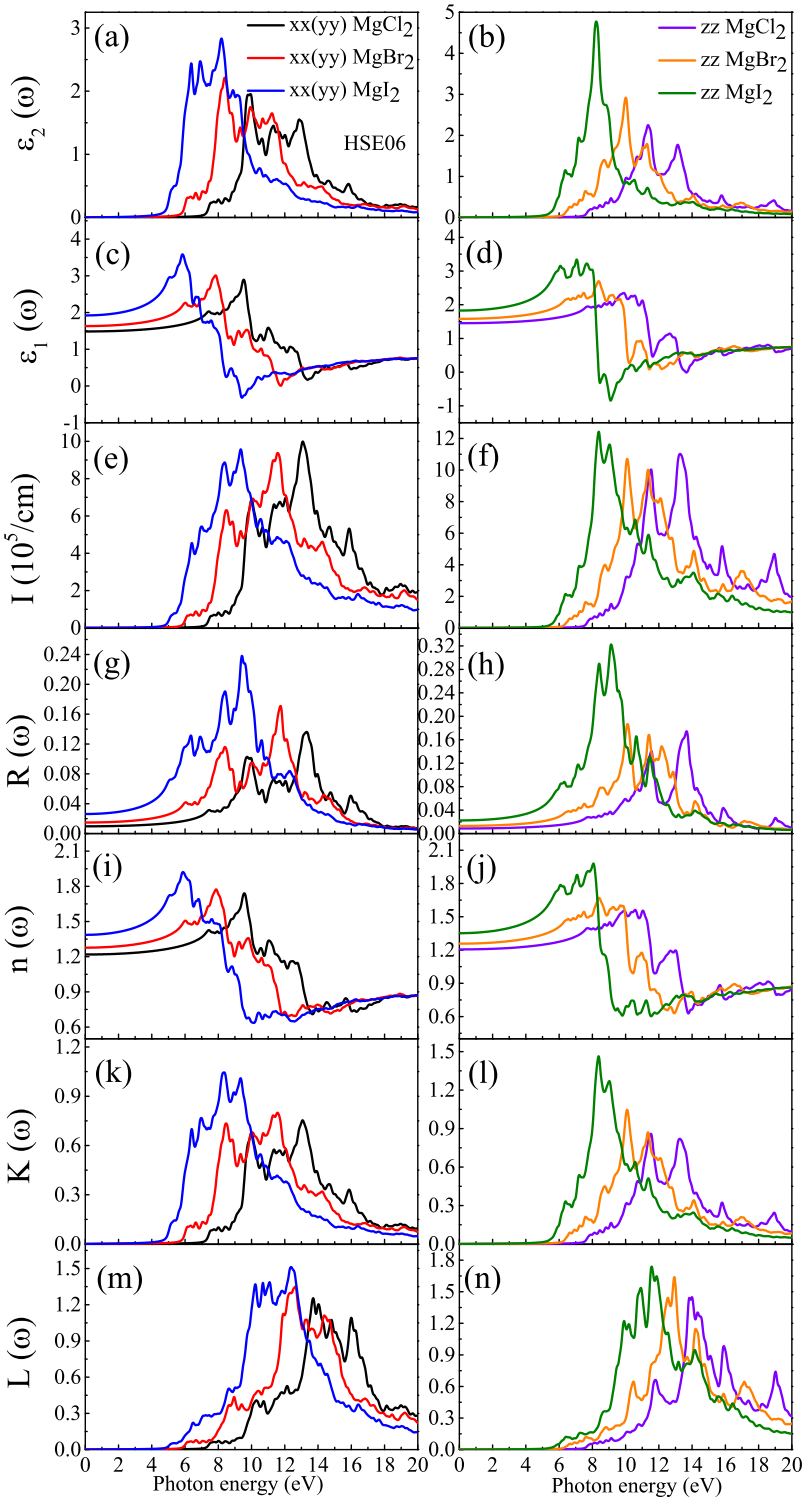

Fig. S4 Optical properties of the monolayer MgX_2 (X = Cl, Br, I). The imaginary $\varepsilon_2(\omega)$ (a, b) and real parts $\varepsilon_1(\omega)$ (c, d) of the complex dielectric function; absorption coefficient I(ω) (e, f); reflectivity R(ω) (g, h); extinction coefficient K(ω)(k,l); refractive index n(ω) (i,j) and energy loss spectrum L(ω) (n, m).

Electronic band structures of SrHX (X=Br,I)

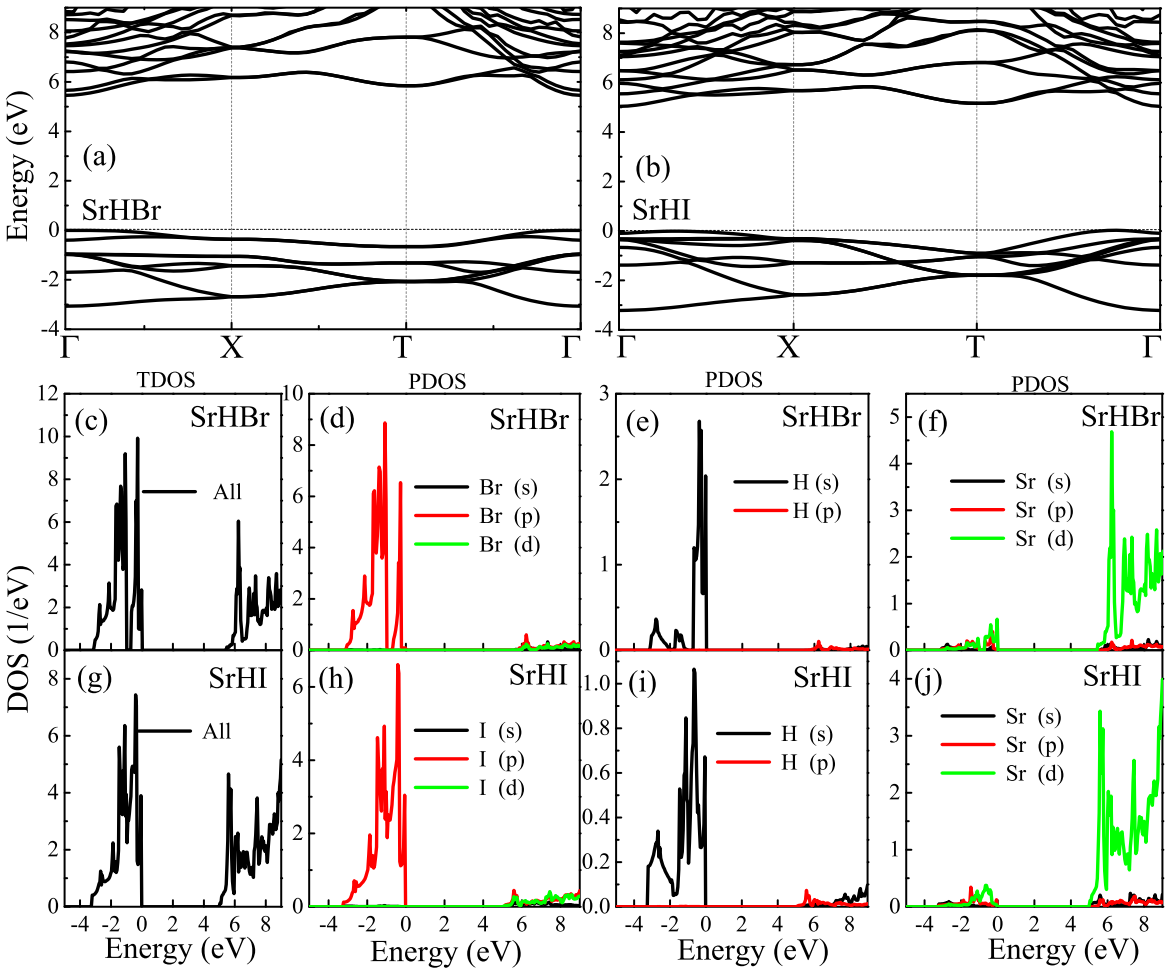

Fig. S5 Electronic band structures of SrHBr (a) and SrHI (b) from HSE06 hybrid functional. TDOS and PDOS for SrHBr (c,d,e,f) and SrHI (g,h,i,j) in the energy range from -5 to 9 eV.

Optical properties of SrHX (X = Br, I) structure

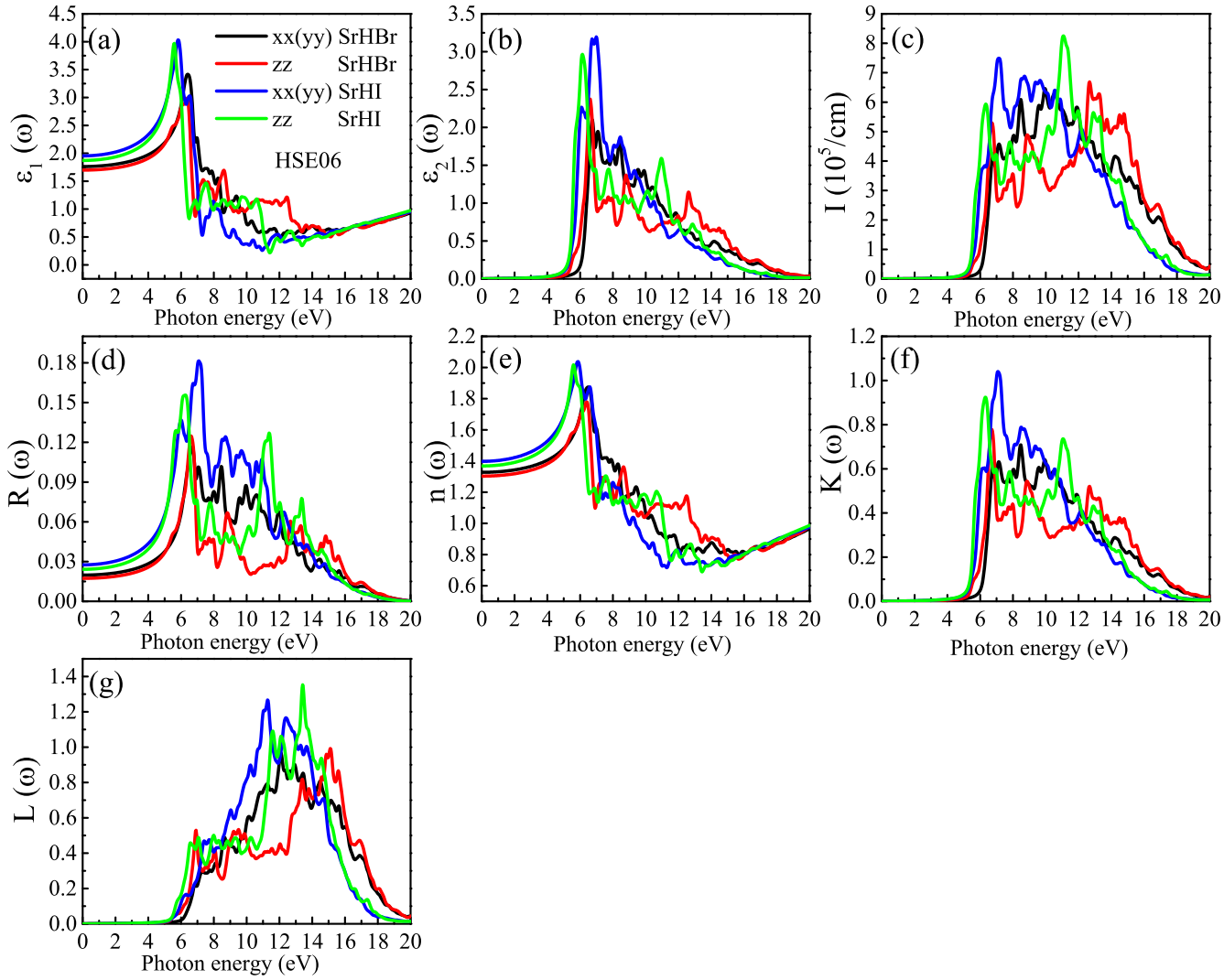

Fig. S6 Optical properties of the monolayer SrHX (X = Br, I). The real $\varepsilon_1(\omega)$ (a) and imaginary parts $\varepsilon_2(\omega)$ (b) of complex dielectric function; absorption coefficient I(ω) (c); reflectivity R(ω) (d); extinction coefficient K(ω)(f); refractive index n(ω) (e) and energy loss spectrum L(ω) (g).

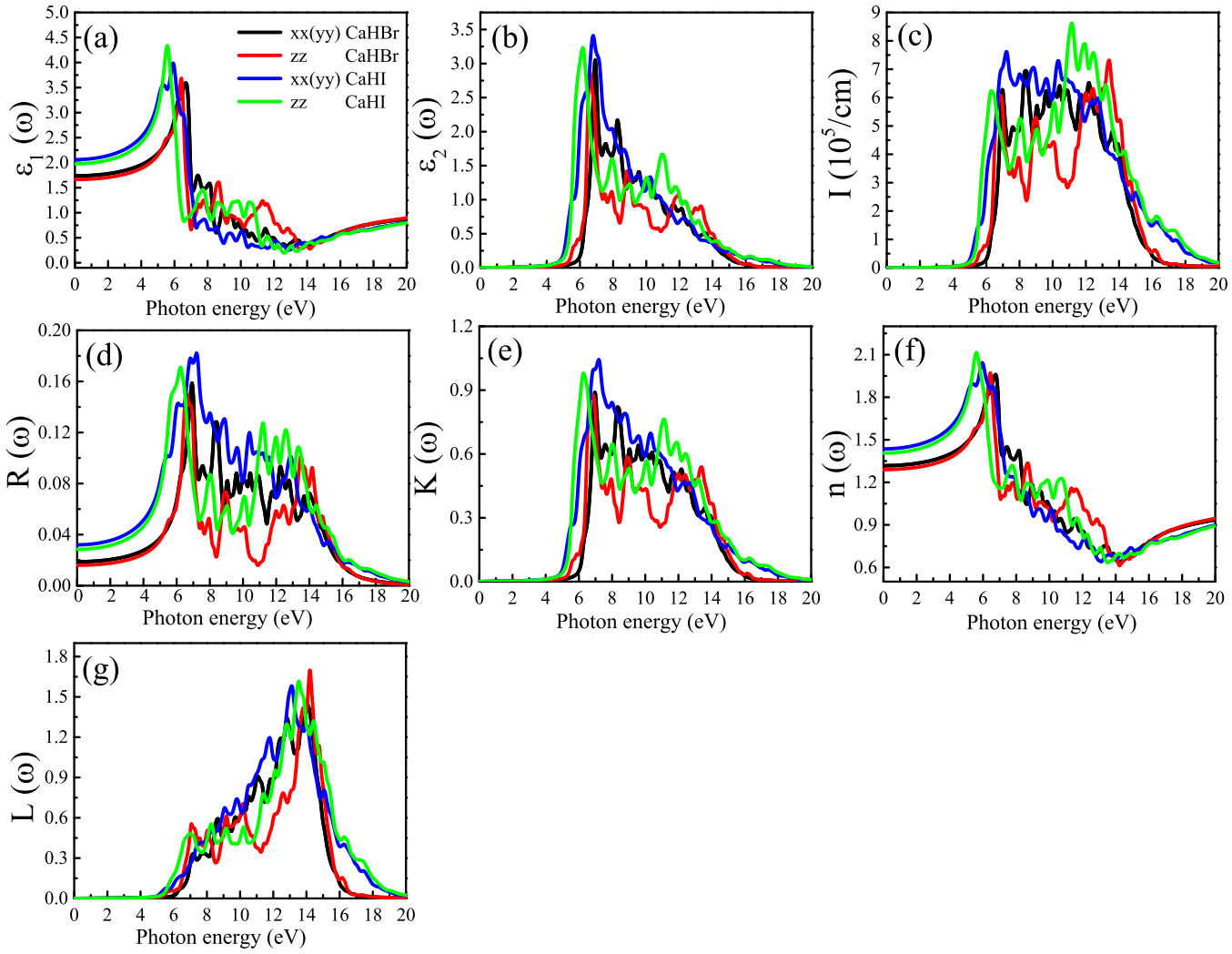

Fig. S7 Optical properties of the monolayer CaHX (X = Cl, I) structure. The real $\varepsilon_1(\omega)$ (a) and imaginary parts $\varepsilon_2(\omega)$ (b) of complex dielectric function; absorption coefficient I(ω) (c); reflectivity R(ω) (d); extinction coefficient K(ω)(e); refractive index n(ω) (f) and energy loss spectrum L(ω) (g).

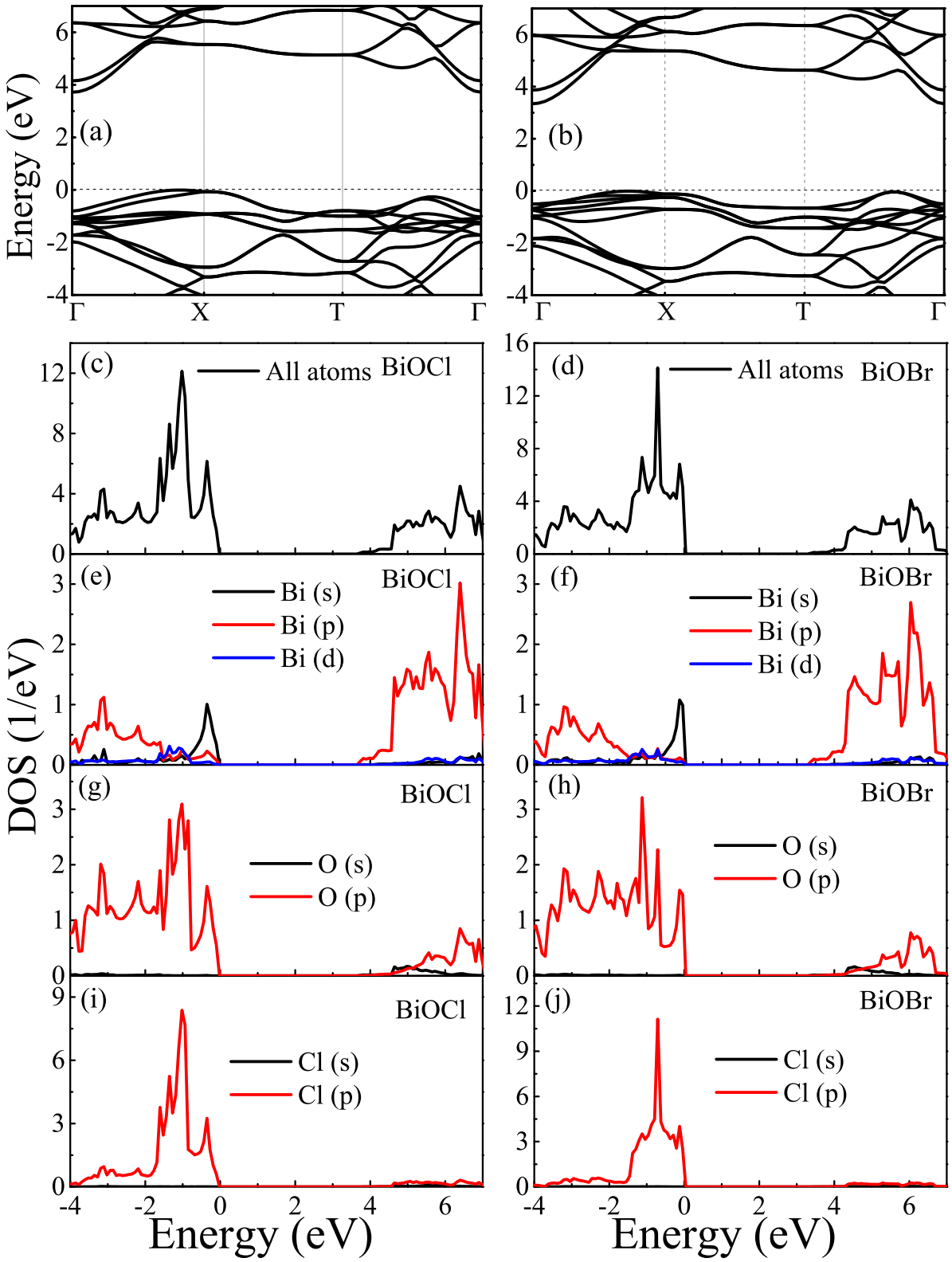

Fig. S8 Electronic band structures of the monolayer BiOCl (X=Cl,Br) using the HSE06 hybrid functional. TDOS and PDOS for BiOCl (X=Cl,Br) in the energy range from -4 to 7 eV.

Optical properties of BiOX (X = Cl, Br) structure

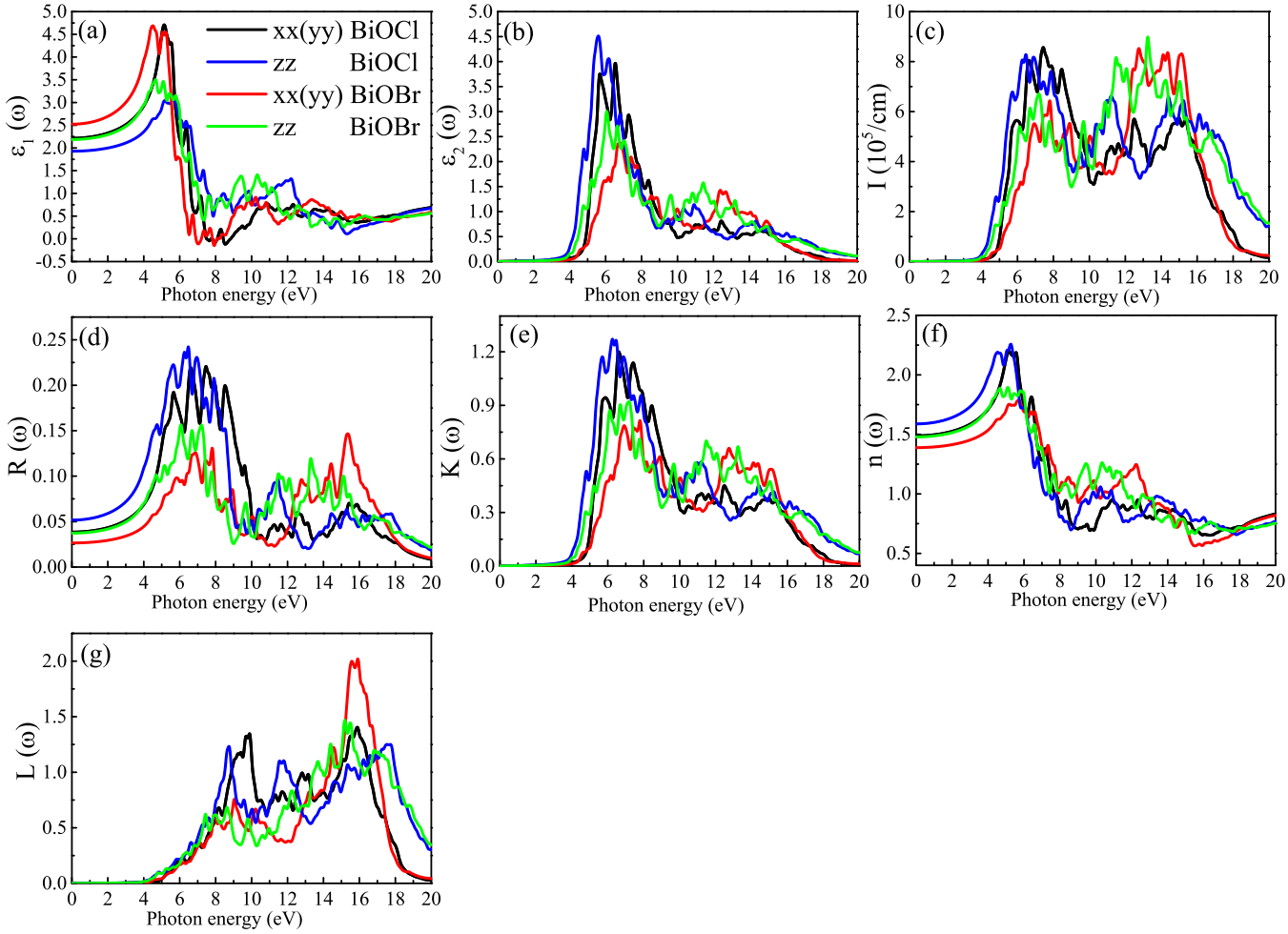

Fig. S9 Optical properties of the monolayer BiOX (X = Cl, Br) structure. The real $\varepsilon_1(\omega)$ (a) and imaginary $\varepsilon_2(\omega)$ parts (b) of complex dielectric function; absorption coefficient I(ω) (c); reflectivity R(ω) (d); extinction coefficient K(ω)(e); refractive index n(ω) (f) and energy loss spectrum L(ω) (g).

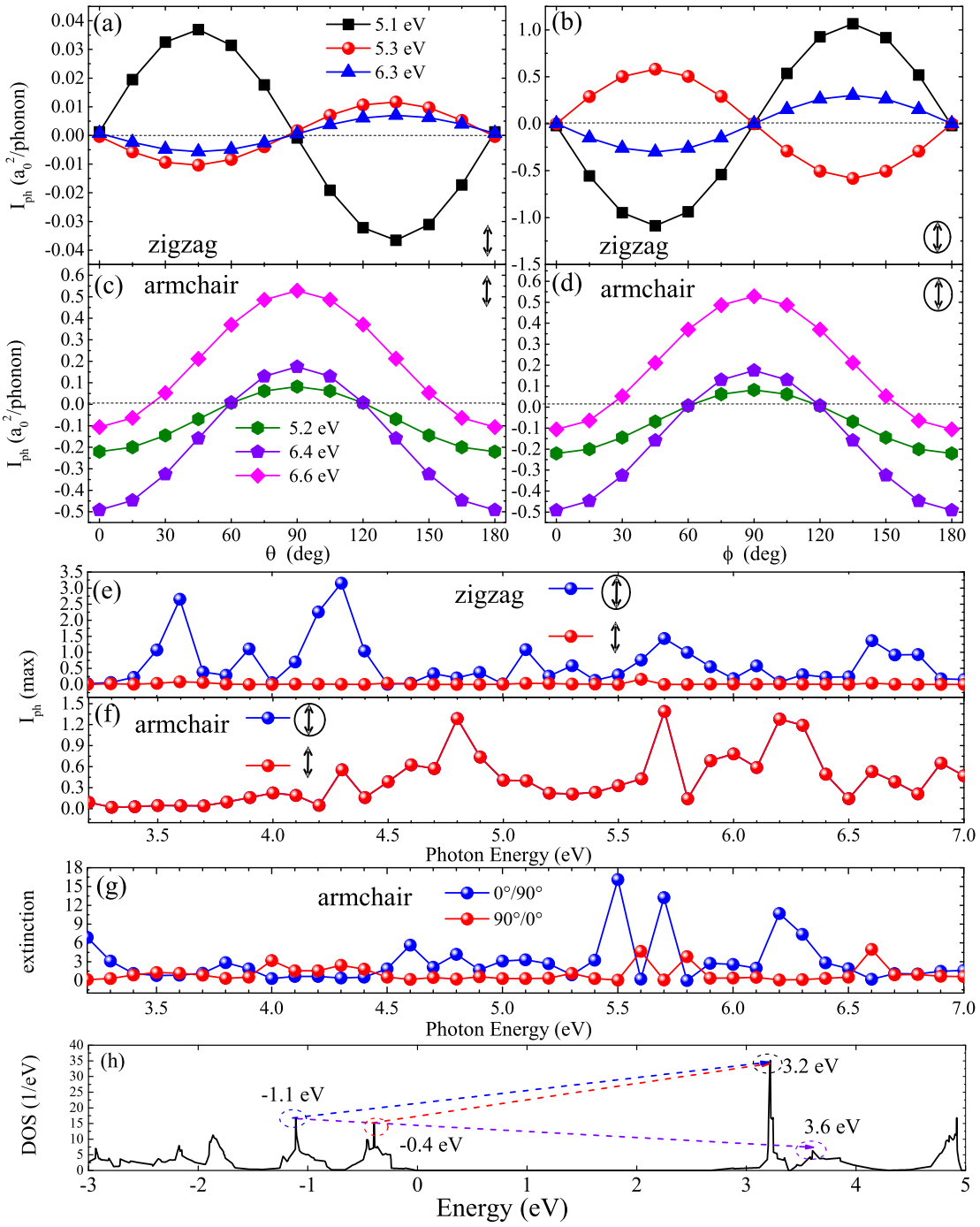

Fig. S10 Photocurrents of the monolayer ZrNBr photodetector at the *normal* incidence of linearly (a, c) and elliptically (b, d) polarized light in the zigzag and armchair directions, respectively. (e, f) Maximum photocurrents for linearly and elliptically polarized light in the zigzag and armchair directions, respectively. (g) Extinction ratios of photocurrents in the armchair direction. DOS of the two-dimensional ZrNBr is shown in (h), where the dashed lines with arrows indicate the electron transition from the valence bands to the conduction bands.

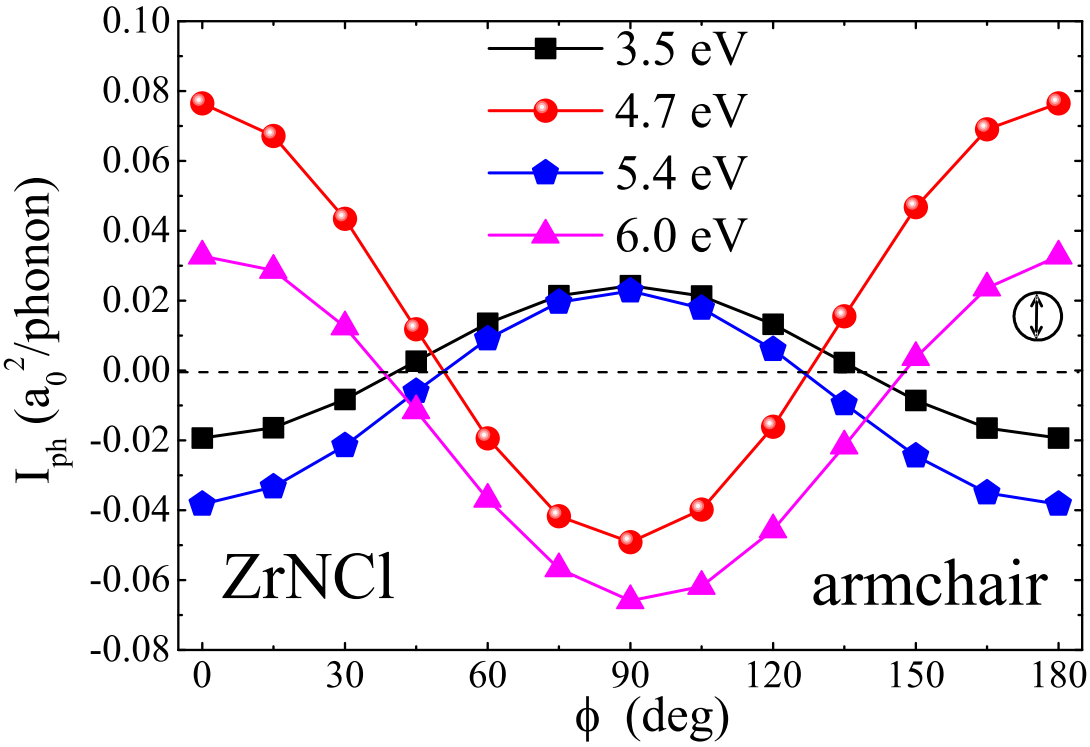

Fig. S11 The photocurrent of the ZrNCl photodetector in the armchair (y) direction under the illumination of elliptically polarized light at *oblique* incidence within the y-z plane.